ELSEVIER

Contents lists available at ScienceDirect

Separation and Purification Technology

journal homepage: www.elsevier.com/locate/seppur



Permeabilities and selectivities in anisotropic planar membranes for gas separations



Juan-Manuel Restrepo-Flóreza, Martin Maldovana, b, s

- ^a School of Chemical & Biomolecular Engineering, Georgia Institute of Technology, Atlanta, GA 30332, USA
- ^b School of Physics, Georgia Institute of Technology, Atlanta, GA 30332, USA

ABSTRACT

The use of membrane technologies for separation processes is an alternative approach to reduce the environmental impact and energy demand of separations. The development of new membrane materials plays a central role to overcome the limitations of membranes in terms of selectivity, permeability, and stability. Most membrane materials in the past have been engineered to control the relative magnitude of the flux of the species diffusing through the membrane. However, mass flux is a vector and controlling its direction can open new opportunities to design separation processes. In this paper we characterize the separation capabilities of metamaterial-inspired anisotropic planar membranes by studying the development of spatially dependent permeabilities and selectivities as a consequence of manipulating the flux direction within the membrane. Specifically, we show how the performance of anisotropic planar membranes for separations can be characterized in terms of permeability, selectivity, and the collected permeate proportion. In contrast to isotropic membrane materials, we show how the selectivity under single stage operation can be increased beyond the selectivities of the constituent materials by reducing the permeate proportion that is collected. Our work provides new opportunities for the design of alternative separation processes that take advantage of flux directional control within membrane materials.

1. Introduction

Alternative separation methods that use reduced amounts of energy are critically needed since separation of chemicals account for a large fraction of the world's energy consumption and CO₂ emissions [1,2]. Highly efficient separation methods hold the promise of improving energy and environmental planning, process economics, and product quality [2-4]. In the last decades, significant attention has been directed towards membrane-based separations due to their lower energy demands. Membrane separations require energies that are generally orders of magnitude smaller than conventional separation operations such as distillation. Such low energy requirement makes membranes ideal candidates to replace dominant energy-intensive separation processes [1,2,4-8]. In recent years, remarkable improvements in fabrication methods have played a major role in the synthesis of new membrane materials with enhanced separation capabilities [3,4,8,9]. Of particular importance has been advances in polymers and molecular sieves [6,10-12]. Despite this significant progress, the selectivities, fouling, and stability properties of membrane materials need to be improved to better leverage their separation capabilities and make them more suitable to general mixtures and separation processes [3-5].

To date most membrane materials are designed on the principle that the membrane needs to selectively allow the passage of one species and reject the other species in the mixture [Fig. 1(a)]. That is, conventional

membranes, although chemically diverse, share a common basic principle for operation: the membrane controls the *flux magnitude* of the species diffusing through the material. We note however that mass flux is a vector and it is certainly possible to move beyond controlling the flux magnitude and to design membrane materials that also manipulate the *flux direction* [13–15]. Importantly, being able to control the direction of flux can provide a new principle for separations where different species are guided to different spatial regions after they cross the membrane [Fig. 1(b) and (c)] [13–15]. We note that manipulating the flux direction within the membrane requires consideration of anisotropic materials, which is in contrast to conventional membranes generally made of isotropic materials. Importantly, the design of anisotropic membrane materials that can direct the diffusion paths of the species and provide a new principle for separations has been largely unexplored.

A starting point for the rational design of anisotropic membrane materials for separations is metamaterials engineering [16–20]. Metamaterials are rationally structured composites with physical properties significantly different from those of their constituent materials [21]. In recent years, metamaterials have been applied to control heat and mass diffusion in diverse engineered structures [14,17,19,21–27]. Inspired by metamaterials theory, we have recently postulated the possibility of designing anisotropic membrane materials that reroute the trajectory of diffusing chemical compounds in a prescribed way [13,15]. In this work

E-mail address: maldovan@gatech.edu (M. Maldovan).

^{*} Corresponding author.

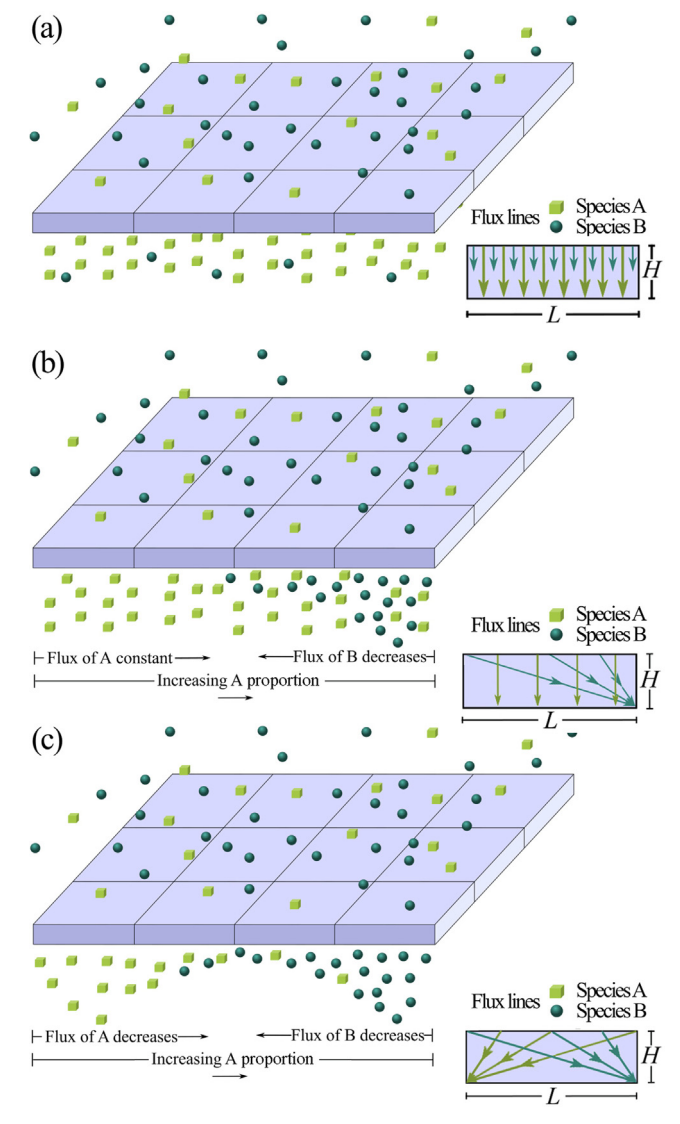


Fig. 1. Schematic representation of a planar membrane. (a) Isotropic membrane: Difference in flux magnitude creates a permeate enriched in species *A*. (b) Anisotropic membrane: the directional control of species *B* towards the right side creates a permeate depleted on species *B* on the left side. (c) Anisotropic membrane: the directional control of both species *A* and *B* creates a permeate in which the flux of *A* is larger on the left and the flux of *B* is larger on the right.

we explore the use of metamaterial-inspired anisotropic planar membranes for the separation of gas mixtures. Gas separations are of particular importance with applications ranging from natural gas sweetening, and CO₂ capture, to the production of highly pure nitrogen used in the microelectronics industry [3,9]. Three common technologies to perform gas separations are cryogenic distillation, pressure swing adsorption (PSA), and membranes [5,28]. Cryogenic distillation is highly energy intensive, while PSA and membranes offer the possibility of reducing the energy demand of the process [5,8,28,29]. Economically, the preferred technology depends fundamentally on the required purity and amount of product [5]. In recent years, advances in the synthesis of membrane materials have broaden the range of applicability of membrane based separation processes [4]. Our work is based on the generalization of Fick's law for anisotropic materials $J_{(i)} = -D_{(i)}\nabla C_{(i)}$, where different components of the diffusivity tensor are rationally designed such that diffusing molecules follow specific trajectories within the membrane. We demonstrate large selectivities for benchmark separations O₂/N₂ and H₂/CH₄ by incorporating anisotropy in separation processes and discuss existing trade-off relations between the variables characterizing the performance of anisotropic membranes: selectivity, permeability, and collected permeate proportion. We show how the introduction of a fundamentally different separation mechanism into the design of membrane materials may provide new avenues to enhance separation capabilities. We study the separation of binary mixtures made of two species A and B by using two different types of anisotropic planar membranes. In the first case, the planar membrane is designed to reroute one of the species in the mixture (e.g. species B) [Fig. 1(b)] while in the second case the membrane simultaneously guides both species A and B [Fig. 1(c)]. The basic goal in both cases is to have species A and B at different spatial areas after they cross the membrane. Importantly, note that the flux of species B in Fig. 1(b) and species A and B in Fig. 1(c) are spatially dependent on the permeate side, i.e. $J_{(i)}(x)$. This is in contrast to isotropic membranes where the fluxes of species A and B are spatially constant under the same conditions (i.e. spatially constant high pressure on the top and low pressure on the bottom) [Fig. 1(a)]. The spatial dependence of the permeate flux $J_{(i)}(x)$ is the fundamental property that will be leveraged to achieve separations.

2. Methods

In this work we study the diffusion of chemical species in anisotropic metamaterial membranes. In anisotropic materials the mass diffusion coefficients are represented by a tensor

$$\overset{\leftrightarrow}{D_{(i)}} = \begin{bmatrix} D_{xx} & D_{xy} \\ D_{yx} & D_{yy} \end{bmatrix}$$
(1)

and the mass diffusion differential equation (i.e. second Fick's law) is given by

$$\frac{\partial C}{\partial t} = -\nabla \cdot J = \nabla \cdot \begin{bmatrix} D_{xx} & D_{xy} \\ D_{yx} & D_{yy} \end{bmatrix} \begin{bmatrix} \partial C/\partial x \\ \partial C/\partial y \end{bmatrix}$$
(2)

where C is the concentration and J is the mass flux. Materials with anisotropic diffusion coefficients are generally not common in nature. Here we design multilayer composites with effective anisotropic properties by making use of effective medium theory (see SI for further details). The governing equation associated with the mass transport processes (Eq. (2)) is difficult to be solved analytically and we thus employ a numerical procedure. Specifically, numerical solutions to mass diffusion processes are obtained with the software COMSOL Multiphysics®, which uses a finite element based approach to solve the mass diffusion differential equation. Importantly, we refine the spatial discretization of the systems such that the resultant numerical predictions are mesh independent. In our simulations, we consider Henry's law (i.e. $C_{(i)s} = p_{(i)}S_{(i)}$ where $C_{(i)s}$ is the interface concentration, $p_{(i)}$ the partial pressure of species i and $S_{(i)}$ the solubility) to establish boundary conditions at the top and bottom boundaries of the membranes and also consider no flux boundary conditions on the sides.

3. Results and discussion

3.1. Rerouting one species (Ideal case)

We first study the separation of A and B by modifying the trajectory of B [Fig. 1(b)], and engineer the membrane anisotropy such that the flux of B is bent to the right as B crosses the membrane. We employ a multilayer structure made of two homogeneous isotropic materials M_1 and M_2 where the plane of the layers is rotated by an angle θ with respect to the direction of the driving force (Fig. 2). Such multilayer structure enables anisotropic mass diffusion due to the different mass diffusion properties along the parallel $\|$ and perpendicular \bot directions to the layers (i.e. parallel and series, respectively). The effective mass diffusion tensor $D_{(i)}$ for multilayer structures is given in SI [27]. Recent advances in layer-by-layer assembly are paving the way toward

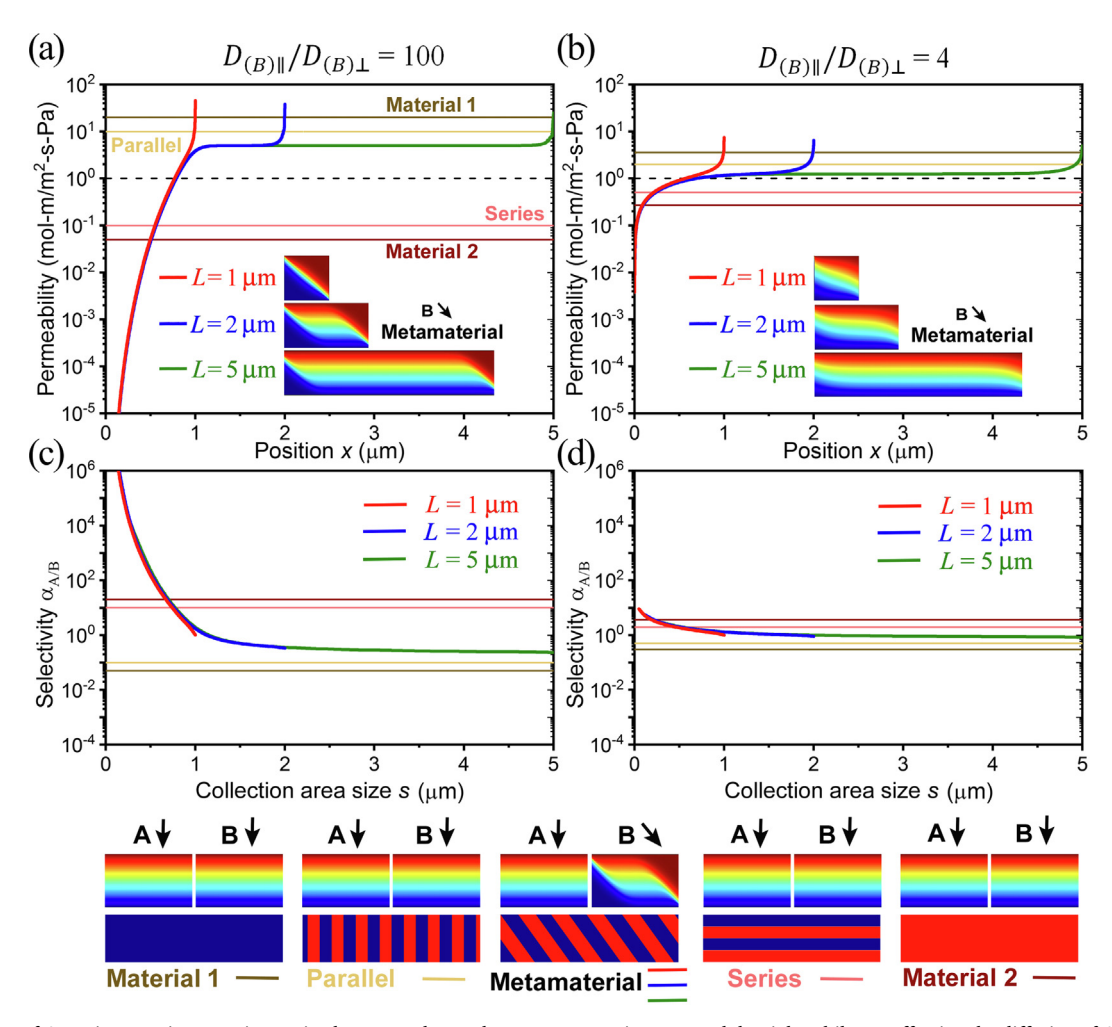


Fig. 2. Separation of *A-B* mixture using an anisotropic planar membrane that reroutes species *B* toward the right while not affecting the diffusion of *A*. Performance of isotropic systems and their series and parallel arrangements are also shown. (a) and (b) Permeability of *B* as a function of *x* for $D_{(B)\parallel}/D_{(B)\perp}=100$ and $D_{(B)\parallel}/D_{(B)\perp}=4$, with $D_{(A)\parallel}/D_{(A)\perp}=1$. (c) and (d) Selectivities $\alpha_{A/B}$ as a function of the length *s* of a collection area on the left side of the membrane. Color maps show concentration of *A* and *B*.

Table 1 Material properties for separation of species A and B (left), and O_2 and N_2 (right). For O_2/N_2 separation M_1 is PDMS and M_2 is PSF. Units $[D] = m^2/s$, $[S] = mol/m^3 Pa$.

Property	A/B separation				O ₂ /N ₂ separation	
	A	В	Α	В	O ₂	N_2
D_{M_1}	1	19.95	1	3.73	3.4×10^{-9}	3.4×10^{-9}
S_{M_1}	1	1	1	1	7.9×10^{-5}	$4.0 imes 10^{-5}$
D_{M_2}	1	0.05	1	0.27	4.4×10^{-12}	1.2×10^{-12}
S_{M_2}	1	1	1	1	1.1×10^{-4}	6.6×10^{-5}
$D_{ }$	1	10	1	2	1.42×10^{-9}	1.28×10^{-9}
$D_{\!\perp}$	1	0.1	1	0.5	1.02×10^{-11}	2.98×10^{-12}
S_{eff}	1	1	1	1	9.45×10^{-5}	5.30×10^{-5}
θ	45	45	45	45	45	45
D_{\parallel}/D_{\perp}	1	100	1	4	139.2	429.5

engineered multilayers for various energy applications, including membranes [30–33]. We first consider that the layered structure is made of two ideal homogeneous isotropic materials M_1 and M_2 whose diffusivities and solubilities are selected such that the membrane modifies only the trajectory of species B to the right. We consider two cases $D_{(B)\parallel}/D_{(B)\perp}=100$ and $D_{(B)\parallel}/D_{(B)\perp}=4$, with $D_{(A)\parallel}/D_{(A)\perp}=1$ (Table 1). We show in Fig. 2(a) and (b) the predicted permeability $P_{(B)}(x)$ for species B as a function of the position x on the permeate side.

The permeability $P_{(i)} = J_{(i)}H/\Delta p_{(i)}$ of species *i* is defined as the flux $J_{(i)}$ times the membrane height H normalized by the driving force $\Delta p_{(i)}$ across the membrane [4,34]. Note that for isotropic membranes $P_{(i)}$ is also equivalent to $D_{(i)}S_{(i)}$. For calculations, we assume a partial pressure of 1 atm on the upper side and complete sweeping on the lower (permeate) side. The height of the membrane is $H = 1 \mu m$ and the lengths are $L=1\,\mu\text{m}$, $2\,\mu\text{m}$, and $5\,\mu\text{m}$. Fig. 2(a) shows the development of a position dependent permeability profile $P_B(x)$ for the controlled species B due to the engineered bending of the trajectory of species B. Specifically, we observe species B depletion on the membrane left side (low local permeability P_B), and enrichment of species B on the right side (high local permeability P_B). Clearly, the magnitude of the depletion of species B on the left side is dependent on the ratio $D_{(B)\parallel}/D_{(B)\perp}$. On the other hand, the permeability P_A of species A remains constant for all positions x on the permeate side since the trajectory of species A is not modified. Importantly, we note that due to the rerouting of species B there exist a spatial area on the permeate side of the membrane (left side) where the permeability of B is dramatically reduced. This lack of species B will be leveraged next to perform separations. To quantify the strong reduction in the permeability of *B* on the left side, we compare in Fig. 2(a) the position-dependent metamaterial permeability $P_B(x)$ against the constant permeabilities corresponding to membranes made of the constituent homogeneous isotropic materials M_1 or M_2 as well as the permeabilities of membranes consisting of series and parallel composite structures made of materials M_1 and M_2 . Note that all the

membranes are operated under the same conditions such that adequate comparisons between the physical effects arising from the use of anisotropic and isotropic membranes can be drawn. Fig. 2(a) shows that, due to thererouting of species B viaanisotropy, the permeability of B on the left side can be orders of magnitude smaller than that corresponding to the constituent materials as well as the series and parallel arrangements.

We next exploit this unconventional permeation behavior to perform the separation of A and B. To obtain a mixture enriched in species A, the area where the products are collected should be on the left side of the membrane (where B is depleted). On the other hand, to obtain a mixture enriched in species B, the collection area should be placed on the right side. Note that in contrast to isotropic membranes, in our anisotropic membranes the selectivity $\alpha_{A/B} = \langle P_{(A)} \rangle / \langle P_{(B)} \rangle$ depends on the size and location of the collection area due to the spatial dependence of the permeability $P_B(x)$. We show in Fig. 2(c) and (d) the selectivities $\alpha_{A/B}$ for the membranes in Fig. 2(a) and (b) for different collection areas on the permeate side. We consider that the collection area starts from the left side of the membrane (i.e. we are interested in a permeate enriched in species A) and we collect the permeate leaving the membrane through the area defined by $0 \le x \le s$, where s is the length of collection area. For a permeate enriched in species B the collection area starts from the right. We find that the ability of the membrane to produce a permeate enriched in the species A significantly increases when the collection area is decreased [Fig. 2(b)]. Importantly, note that depending on the size of the area where the permeate is collected, it is possible to achieve selectivities $\alpha_{A/B}$ that are orders of magnitude larger than those of the constituent homogeneous isotropic materials as well as the series and parallel composite structures. These large selectivities $\alpha_{A/B}$ are a consequence of the low permeability of B on the left side of the membrane due to anisotropy.

We note that as the collection area is reduced on the permeate side in order to obtain high selectivities one is reducing the collected permeate proportion (CPP) which is given by $CPP = \int_0^s J_{(i)}(x) dx / \int_0^L J_{(i)}(x) dx$. Note that in conventional isotropic membranes, the entire permeate fraction (with spatially constant composition on the permeate side of the membrane) is collected and thus CPP = 1. On the contrary, in anisotropic membrane materials, selecting the size of the collection area is critical to incorporate the advantages of flux directional control and enhanced selectivities, therefore CPP < 1. In other words, anisotropic membranes enable a novel property since one can increase the selectivity while reducing the CPP under single stage operation (note there are no intermediate pressures in our membrane), which is contrast to isotropic membranes. Note that if the collection area comprises the entire anisotropic membrane on the permeate side, there is no advantage in rerouting the flux lines and the permeate composition obtained lies between the limits imposed by the constituent materials [Fig. 2(c) and (d), for x = L].

3.2. Rerouting one species (Real case)

After studying separation of mixtures by ideal anisotropic planar membranes, we next focus on a real separation process and study the permeability and selectivity of oxygen and nitrogen through anisotropic membranes made of realistic materials. To achieve different anisotropic properties for the diffusion of oxygen and nitrogen [15], we consider layered membranes made of PDMS [35] and PSF [36] (Table 1). In Fig. 3(a)–(c) we show the predicted permeability for nitrogen $P_{\rm N_2}(x)$ and oxygen $P_{\rm O_2}(x)$ as a function of the position x along the membrane on the permeate side, as well as the selectivities $\alpha_{\rm O_2/N_2}$ as a function of the size of the collection area. In contrast with the idealized systems discussed in the first part of this work, in this case, the diffusion paths of the two species are influenced by the anisotropic membrane. That is, for the realistic material case under study, the trajectories of both oxygen and nitrogen are modified by the anisotropic membrane and the species

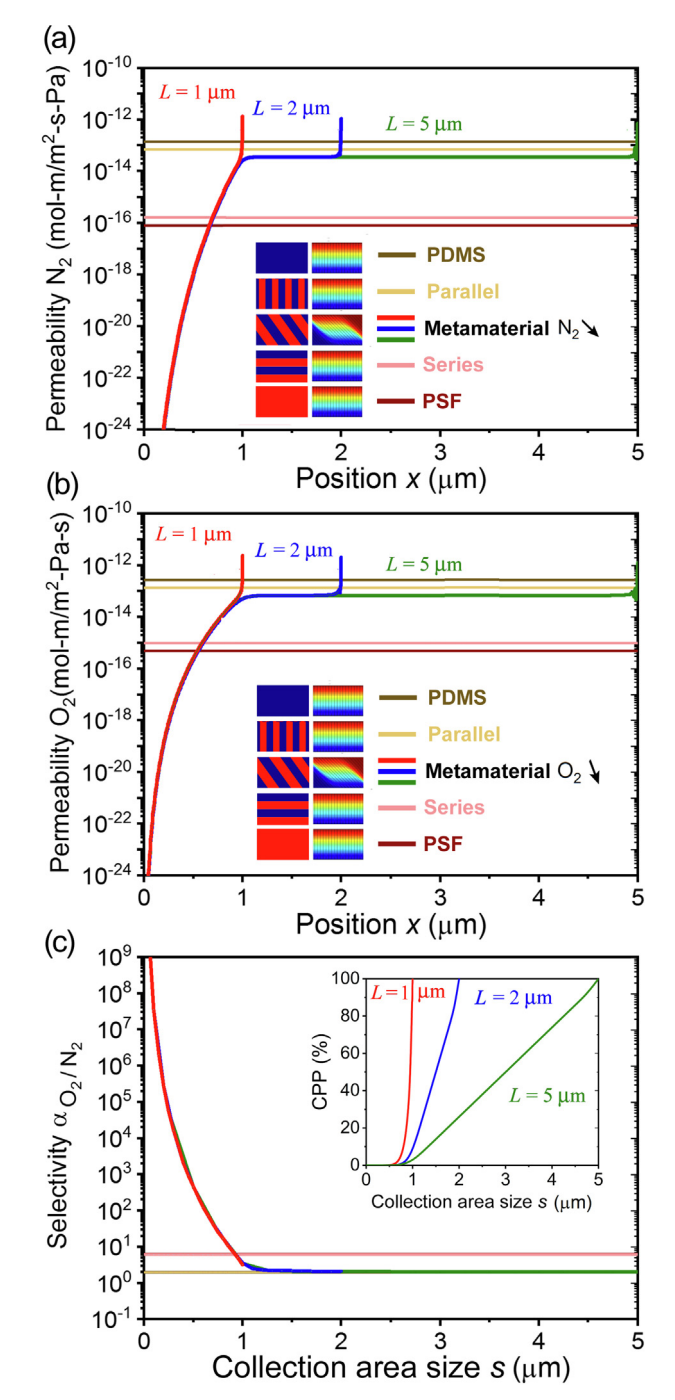


Fig. 3. Separation of a binary mixture of O_2 and N_2 using an anisotropic planar membrane that preferentially reroutes N_2 to the right. (a) and (b) Permeabilities of N_2 and O_2 as a function of the position x on the permeate side. (c) Selectivity α_{O_2/N_2} as a function of the length s of a collection area placed at the left side of the membrane. Inset shows collected permeate proportion (*CPP*).

are rerouted toward the right edge. Note however that the rerouting is more pronounced for nitrogen since $P_{\rm N_2}(x) < P_{\rm O_2}(x)$ on the left side. We show in Fig. 3(c) that the preferential rerouting of nitrogen toward the right side causes a significant increase in the oxygen selectivity $\alpha_{\rm O_2/N_2}$ when the collection area is located at the left side of the membrane. Importantly, the selectivity of the anisotropic membrane can be made larger than the selectivities of the isotropic materials comprising the membrane. In fact the selectivity values obtained in this work are orders of magnitude higher that those obtained with any other available material. As mentioned previously, the obtained selectivities are

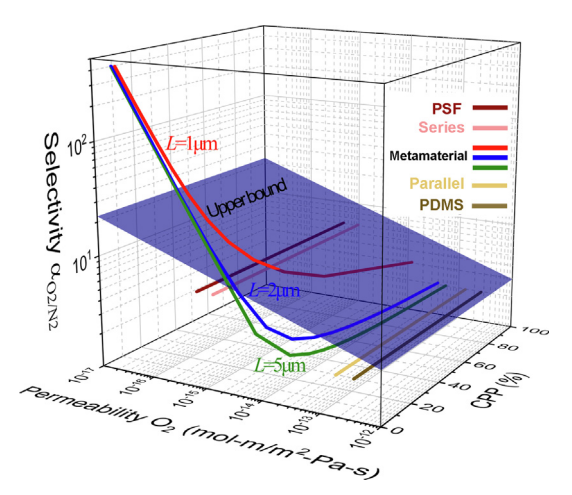


Fig. 4. Modified Robeson plot for the separation of O_2 and N_2 using an anisotropic planar membrane. The plot shows the relation between the selectivity, permeability, and *CPP*.

correlated to the *CPP* which is shown in Fig. 3(c)-inset. The relation between permeability, selectivity, and *CPP* for the separation of oxygen and nitrogen using an anisotropic membrane material made of layered PDMS and PSF materials is shown in Fig. 4. This representation is a 3D expansion of the Robeson plot allowing for a complete characterization of the anisotropic membrane [37,38]. Note that in this plot it is possible to compare the performance of anisotropic materials, isotropic materials, and the upper bound. Isotropic materials have fixed selectivity vs. permeability values. On the other hand, the upper bound for isotropic materials appears as a plane [37,38]. Fig. 4 clearly shows the trade-off

Table 2 Material properties for separation of species A and B (left), and H_2 and CH_4 (right), which are designed to independently control the diffusion trajectory of the two species. For H_2/CH_4 separation M_1 is PTMSP, M_2 PDMS, M_3 PIM-7, and M_4 PMDA-BATPHF. Units $[D] = m^2/s$, $[S] = mol/m^3$ Pa.

Property	A/B separation		H ₂ /CH ₄ separation		
	A	В	H_2	CH ₄	
D_{M_1}	19.95	19.95	2.60×10^{-8}	3.60×10^{-9}	
S_{M_1}	1	1	1.74×10^{-4}	1.25×10^{-3}	
D_{M_2}	0.05	19.95	1.29×10^{-8}	2.17×10^{-9}	
S_{M_2}	1	1	1.98×10^{-5}	1.67×10^{-4}	
D_{M_3}	19.95	0.05	1.10×10^{-9}	5.10×10^{-12}	
S_{M_3}	1	1	2.41×10^{-4}	3.62×10^{-3}	
D_{M_4}	0.05	0.05	2.20×10^{-10}	6.90×10^{-13}	
S_{M_4}	1	1	6.94×10^{-5}	4.22×10^{-4}	
$D_{ }$	0.1	10	2.03×10^{-9}	2.45×10^{-10}	
$D_{\! \perp}$	10	0.1	2.10×10^{-9}	1.37×10^{-11}	
S_{eff}	1	1	1.26×10^{-4}	1.40×10^{-3}	
θ	45	45	45	45	
D_{\parallel}/D_{\perp}	0.01	100	1.05	0.056	

between selectivity α and CPP, which is a property exclusive of anisotropic membranes. Note that in isotropic membranes made of PDMS, PSF or their series and parallel combinations, a reduction in the CPP does not cause an increase in the selectivity. These results demonstrate the novel properties of anisotropic membranes in terms of selectivity values that depend on the area where the products are recovered, and more importantly, achieving enhanced selectivities beyond the values of corresponding to the constituent materials.

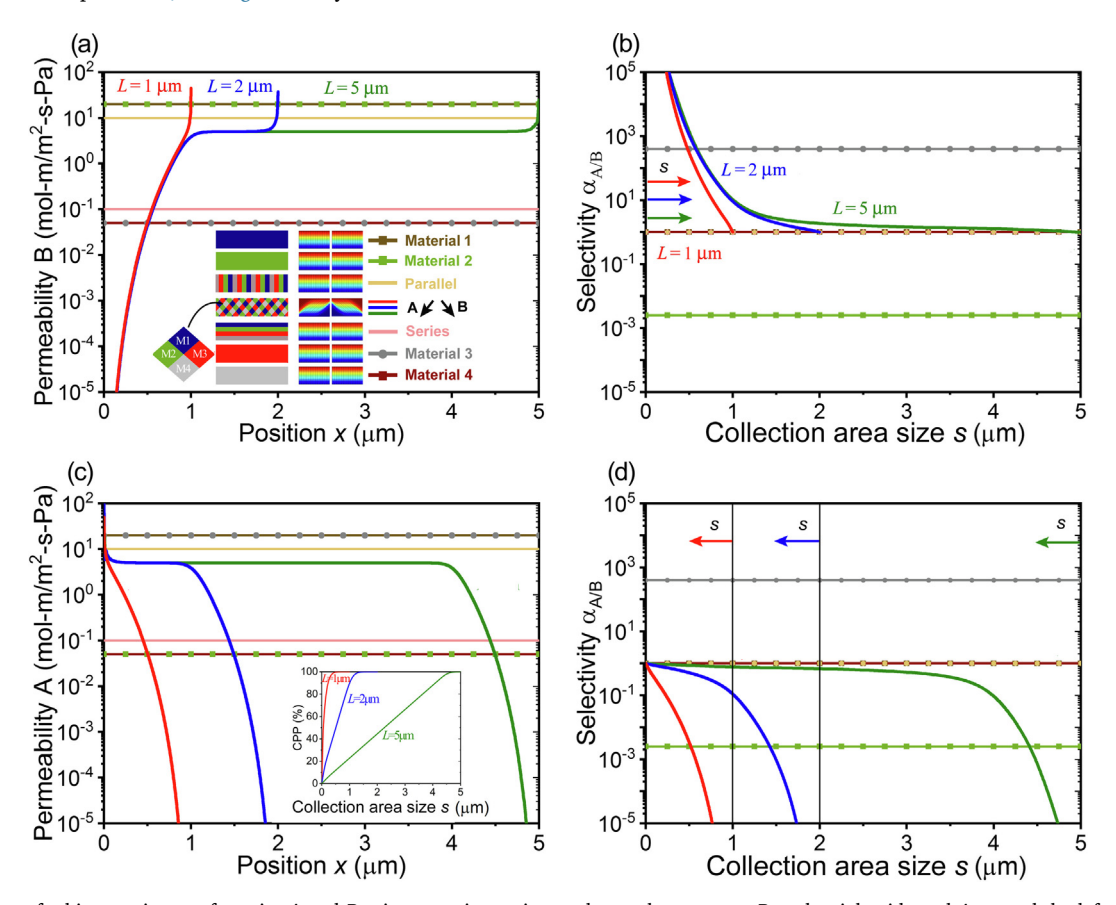


Fig. 5. Separation of a binary mixture of species A and B using an anisotropic membrane that reroutes B to the right side and A toward the left side. (a) and (b) Permeabilities of A and B as a function of the position on the permeate side. (c) and (d) Selectivities $\alpha_{A/B}$ as a function of the length s of a collection area placed at the left side (c) and right side (d) of the membrane. Inset: CPP of species A as a function of the length s of a collection area placed at the left side of the membrane.

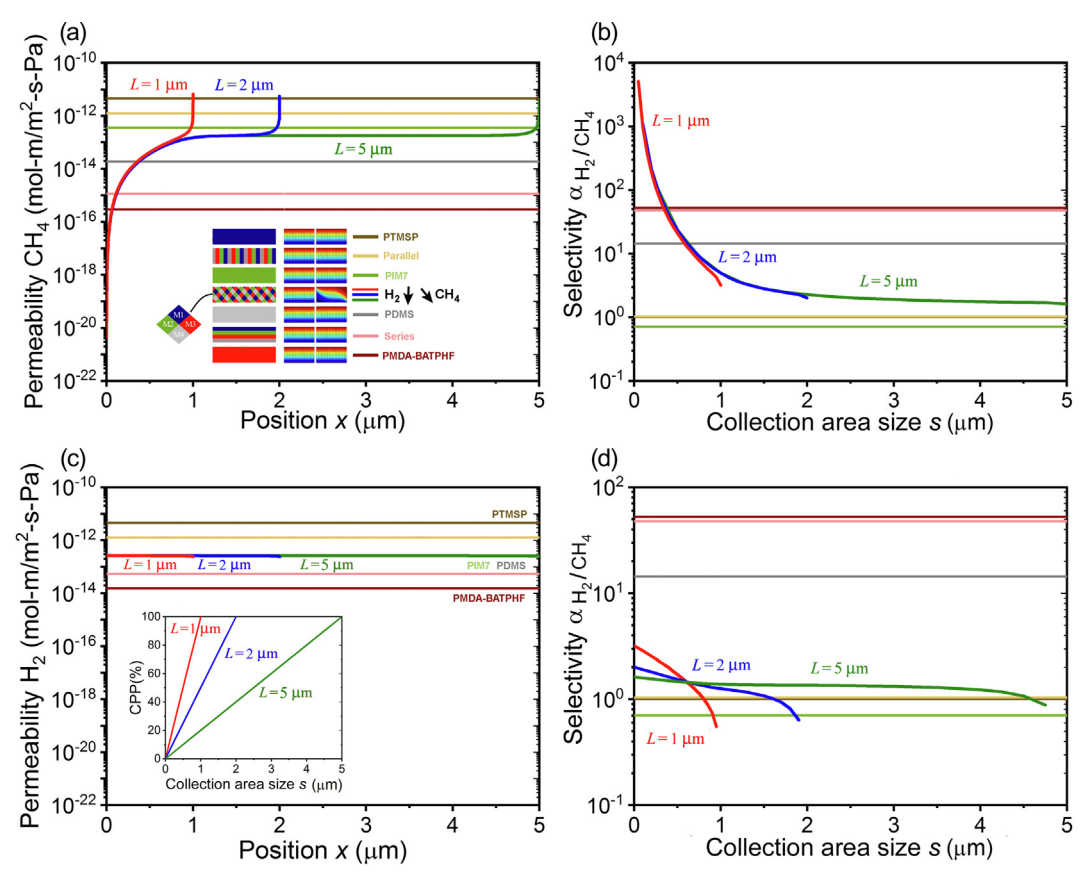


Fig. 6. Separation of H_2 and CH_4 in a planar membrane that reroutes CH_4 to the right side and H_2 to the left side. (a) and (b) Permeability of CH_4 and H_2 as a function of the position x on the permeate side. (c) and (d) Ideal selectivity α_{H_2/CH_4} as a function of the length s of a collection area placed at the left (c) and right (d) side of the membrane. Inset: CPP of H_2 as a function of the length s of a collection area placed at the left.

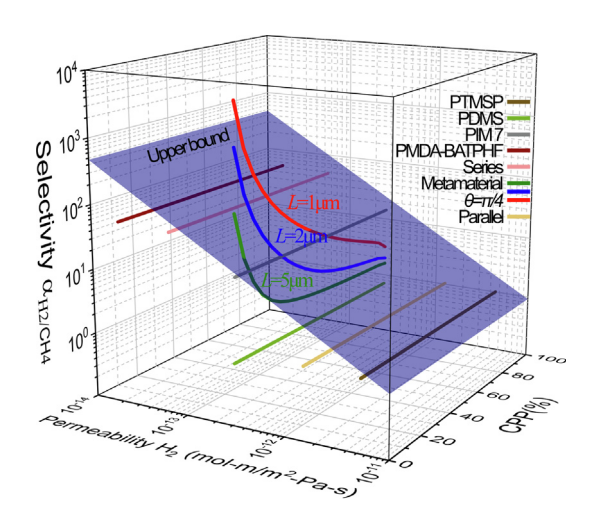


Fig. 7. Modified Robeson plot for the separation of N_2 and CH_4 using an anisotropic planar membrane. The plot shows the relation between the selectivity, permeability, and CPP.

3.3. Rerouting two species (Ideal case)

We also study the permeability and selectivity of anisotropic planar membranes that manipulate the diffusion paths of both species A and B [13]. Specifically, we consider planar membranes made of materials M_1 , M_2 , M_3 and M_4 spatially arranged as shown in Fig. 5(a), which allows to reroute species A and B toward opposite directions after they cross the membrane. The diffusivities along each principal axis $D_{(i)\parallel}$ and $D_{(i)\perp}$ are obtained by using a resistors network analogy (see SI). The

material properties are presented in Table 2. Importantly, note that in this case we have $D_{(A)\parallel}/D_{(A)\perp}<1$ and $D_{(B)\parallel}/D_{(B)\perp}>1$, allowing us to reroute species A and B toward different places. Fig. 5(a) and (b) show the permeabilities $P_A(x)$ and $P_B(x)$ as a function of the position on the permeate side, where it can be seen how the species A is depleted near the right edge (low $P_A(x)$) and the species B is depleted near the left (low $P_R(x)$). That is, species A is directed to the left while species B is directed to the right. These opposite trends cause an interesting result in terms of selectivities. If one collects the permeate near the left side, the membrane is selective in species A [Fig. 5(c)]. On the other hand, if one collects near the right side the membrane is selective in species B [Fig. 5(d)]. Note that in contrast to the case where only B was rerouted, in this case the membrane is able to achieve selectivities that are higher than any of the constituent materials for both species A [Fig. 5(c)] and species B [Fig. 5(d)]. This is a consequence of the development of simultaneous spatially-dependent permeability profiles for A and B, where $P_A(x)$ is low on the right and $P_B(x)$ is low on the left. Another important advantage of this anisotropic planar membrane is the increase in the CPP factor, note that if only B is rerouted, a linear CPP vs collection area is established. In contrast, we see in Fig. 5(c) that by rerouting the two species yields a non-linear profile. The increase is a direct consequence of the additional rerouting to species A toward the collection area.

3.4. Rerouting two species (Real case)

In Fig. 6 we study the performance of the proposed structure for the separation of a binary mixture of $\rm H_2$ and $\rm CH_4$. In this case, the anisotropic membrane is made of PTMSP [39], PDMS [35], PIM-7 [40] and PMDA-BATPHF [41] (Table 2). These materials have been selected such that the effective medium has $D_{\rm (H_2)\parallel}/D_{\rm (H_2)\perp}>1$ and

 $D_{(CH_4)\parallel}/D_{(CH_4)\perp} < 1$, and CH₄ is rerouted to the right and H₂ to the left side of the membrane. The permeability profiles shown in Fig. 6(a) and (b) show that in the membrane made of realistic materials CH₄ (species B) is detoured toward the right side and H₂ (species A) essentially moves in the vertical direction. This effect is significant since it proves that independent control of the trajectory of diffusing molecules can be obtained in our membrane (e.g. we reroute CH4 to the right without affecting H2). In terms of CPP of H2, note that the dependence with respect to the collection area size [Fig. 6(c), inset] follows a nearly linear dependence. This result is in sharp contrast with the case of O₂ separation [Fig. 3(c), inset] where the CPP is non-linear with respect to the collection area size. This is because in the present case. H₂ is not being rerouted to the right side. A summary of the relation between selectivity, permeability, and CPP is shown in Fig. 7 where we can observe the described trade-off between selectivity and CPP. Additionally, it is also possible to observe that in contrast to Fig. 4 there is not a significant change in the permeability of the membrane when the CPP is reduced, i.e. when the collection area decreased. This is also a consequence of the fact that H₂ is not being rerouted to the right side.

4. Conclusions

In summary, we presented a complete framework for the characterization of anisotropic planar materials for gas separations. We used metamaterials theory to design and study anisotropic planar membrane materials in which the flux direction of the species is controlled as the species diffuse within the membrane. We showed that the incorporation of this new physical mechanism leads to significant changes in the performance of the membrane. Due to the development of spatially-dependent permeability profiles, we found selectivities that are larger than the selectivities of the constituent materials and corresponding series and parallel models under single stage operation. Our results also show the existence of a trade-off relation between the selectivity and the collected permeate proportion for anisotropic planar membranes, a relation that is absent for isotropic membranes in single stage operation.

Acknowledgments

This work is supported by the National Science Foundation [Grant No. 1744212].

Appendix A. Supplementary material

Supplementary data to this article can be found online at https://doi.org/10.1016/j.seppur.2019.115762.

References

- D.S. Sholl, R.P. Lively, Seven chemical separations to change the world, Nature 532 (2016) 435–437.
- [2] Oak Ridge National Laboratory, Materials for separation technologies: energy and emission reduction opportunities, Oak Ridge, 2005.
- [3] R.W. Baker, B.T. Low, Gas separation membrane materials: a perspective, Macromolecules 47 (2014) 6999–7013.
- [4] W.J. Koros, C. Zhang, Materials for next-generation molecularly selective synthetic membranes, Nat. Mater. 16 (2017) 289–297.
- [5] R.W. Baker, Membrane Technology and Applications, 3rd ed., John Wiley & Sons Inc, 2012.
- [6] W.J. Koros, R.P. Lively, Water and beyond: expanding the sectrum of large-scale energy efficient separation processes, AIChE J. 58 (2012) 2624–2633.
- [7] M.L. Jue, R.P. Lively, Targeted gas separations through polymer membrane functionalization, React. Funct. Polym. 86 (2015) 40–43.

- [8] D.F. Sanders, Z.P. Smith, R. Guo, L.M. Robeson, J.E. McGrath, D.R. Paul, B.D. Freeman, Energy-efficient polymeric gas separation membranes for a sustainable future: a review, Polymer 54 (2013) 4729–4761.
- [9] P. Bernardo, E. Drioli, G. Golemme, Membrane gas separation: a review/state of the art, Ind. Eng. Chem. Res. 48 (2009) 4638–4663.
- [10] M.G. Buonomenna, W. Yave, G. Golemme, Some approaches for high performance polymer based membranes for gas separation: block copolymers, carbon molecular sieves and mixed matrix membranes, RSC Adv. 2 (2012) 10745–10773.
- [11] C.M. Zimmerman, A. Singh, W.J. Koros, Tailoring mixed matrix composite membranes for gas separations, J. Memb. Sci. 137 (1997) 145–154.
- [12] W.J. Koros, G.K. Fleming, S.M. Jordan, T.H. Kim, H.H. Hoehn, Polymeric membrane materials for solution-diffusion based permeation separations, Prog. Polym. Sci. 13 (1988) 339–401.
- [13] J.-M. Restrepo-Flórez, M. Maldovan, Metamaterial membranes, J. Phys. D. Appl. Phys. 50 (2017) 25104.
- [14] J.M. Restrepo-Flórez, M. Maldovan, Mass separation by metamaterials, Sci. Rep. 6 (2016) 21971.
- [15] J.-M. Restrepo-Flórez, M. Maldovan, Breaking separation limits in membrane technology, J. Memb. Sci. 566 (2018) 301–306.
- [16] J.B. Pendry, D. Schurig, D.R. Smith, Controlling electromagnetic fields, Science 80 (312) (2006) 1780–1782.
- [17] S. Guenneau, T.M. Puvirajesinghe, Fick's second law transformed: one path to cloaking in mass diffusion, J. R. Soc. Interf. 10 (2013) 20130106.
- [18] S. Guenneau, C. Amra, D. Veynante, Transformation thermodynamics: cloaking and concentrating heat flux, Opt. Exp. 20 (2012) 8207–8218.
- [19] S. Narayana, Y. Sato, Heat flux manipulation with engineered thermal materials, Phys. Rev. Lett. 108 (2012) 214303.
- [20] M. Maldovan, Sound and heat revolutions in phononics, Nature 503 (2013) 209–217.
- [21] M. Kadic, T. Bückmann, R. Schittny, M. Wegener, Metamaterials beyond electromagnetism, Rep. Prog. Phys. 76 (2013) 126501.
- [22] S. Guenneau, D. Petiteau, M. Zerrad, C. Amra, T. Puvirajesinghe, Transformed Fourier and Fick equations for the control of heat and mass diffusion, AIP Adv. 5 (2015) 053404.
- [23] R. Schittny, M. Kadic, S. Guenneau, M. Wegener, Experiments on transformation thermodynamics: molding the flow of heat. Phys. Rev. Lett. 110 (2013) 195901.
- [24] E.M. Dede, T. Nomura, J. Lee, Thermal-composite design optimization for heat flux shielding, focusing, and reversal, Struct. Multidiscip. Optim. 49 (2014) 59–68.
- [25] L. Zeng, R. Song, Controlling chloride ions diffusion in concrete, Sci. Rep. 3 (2013)
- [26] J.M. Restrepo-Flórez, M. Maldovan, Rational design of mass diffusion metamaterial concentrators based on coordinate transformations, J. Appl. Phys. 120 (2016) 084902
- [27] J.M. Restrepo-Flórez, M. Maldovan, Mass diffusion cloaking and focusing with metamaterials, Appl. Phys. Lett. 111 (2017) 071903.
- [28] A.R. Smith, J. Klosek, A review of air separation technologies and their integration with energy conversion processes, Fuel Process. Technol. 70 (2001) 115–134.
- [29] K. Seshan, Pressure swing adsorption, Ind. Eng. Chem. Res. 41 (2002) 1389-1392.
- [30] J.J. Richardson, M. Björnmalm, F. Caruso, Technology-driven layer-by-layer assembly of nanofilms, Science 80 (2015) 348.
- [31] A.R. Ajitha, M.K. Aswathi, M. H.J., J. Izdebska, S. Thomas, Multicomponent polymeric materials, Springer, Dordrecht, 2016.
- [32] M. Ponting, A. Hiltner, E. Baer, Polymer nanostructures by forced assembly: process, structure, and properties, Macromol. Symp. 294 (2010) 19–32.
- [33] M. Gupta, Y. Lin, T. Deans, E. Baer, A. Hiltner, D.A. Schiraldi, Structure and gas barrier properties of poly (propylene-graft-maleic anhydride)/phosphate glass composites prepared by microlayer coextrusion, Macromolecules 43 (2010) 4230–4239.
- [34] H.B. Park, J. Kamcev, L.M. Robeson, M. Elimelech, B.D. Freeman, Maximizing the right stuff: the trade-off between membrane permeability and selectivity, Science 356 (2017) eab0530.
- [35] T.C. Merkel, V.I. Bondar, K. Nagai, B.D. Freeman, I. Pinnau, Gas sorption, diffusion, and permeation in poly(dimethylsiloxane), J. Polym. Sci. Part B Polym. Phys. 38 (2000) 415–434.
- [36] J.S. McHattie, W.J. Koros, D.R. Paul, Gas transport properties of polysulfones: 1. Role of symmetry of methyl group placement on bisphenol, Polymer 32 (1991) 840–850
- [37] L.M. Robeson, The upper bound revisited, J. Memb. Sci. 320 (2008) 390–400.
- [38] L.M. Robeson, Correlation of separation factor versus permeability for polymeric membranes, J. Memb. Sci. 62 (1991) 165–185.
- [39] T.C. Merkel, V. Bondar, K. Nagai, B.D. Freeman, Perfluorocarbon gases in poly (1-trimethylsilyl-1-propyne), J. Polym. Sci. Part B Polym. Phys. 38 (2000) 273–296.
 [40] P.M. Budd, K.J. Msayib, C.E. Tattershall, B.S. Ghanem, K.J. Reynolds,
- N.B. McKeown, D. Fritsch, Gas separation membranes from polymers of intrinsic microporosity, J. Memb. Sci. 251 (2005) 263–269.
- [41] K. Tanaka, H. Kita, M. Okano, K. Okamoto, Permeability and permselectivity of gases in fluorinated and non-fluorinated polyimides, Polymer 33 (1992) 585–592.